

The Force Convection Heat Transfer of A Nanofluid Over A Flat Plate: Using The Buongiorno's Model: The Thermophysical Properties As A Function of Nanoparticles

Mahmoud Sabour and Mohammad Ghalambaz

Department of Mechanical Engineering, Dezful Branch, Islamic Azad University, Dezful, Iran

ABSTRACT

A drift-flux model is utilized to theoretically analyze the boundary layer flow and heat transfer of a nanofluid over a flat plate. The concentration of nanoparticles at the plate is obtained using the solution of the governing equations. Assuming a fixed magnitude of free stream velocity, the results show that the heat transfer may enhance up to 22% or decrease about -7% by using nanofluids compared to the pure base fluid.

KEYWORDS

Nanofluid; Drift-flux, Zero mass flux, Force Convection.

1. INTRODUCTION

The nanofluids are new-engineered fluids with enhanced thermo-physical properties. Nanofluids are produced by suspending nanoparticles in a conventional base fluid. The experimental measurements of nanofluids indicate augmentation of the thermal conductivity and viscosity of nanofluids even with small volume fraction of nanoparticles [1-3]. Therefore, the addition of small amount of nanoparticles to a conventional heat transfer fluids may significantly enhance the convective heat transfer of the host fluid. An excellent review of the practical applications of nanofluids can be found in a recent review by Saidur *et al.* [4].

An increase of the volume fraction of nanoparticles would increase the thermal conductivity of nanofluids, which is expected to enhance the convective heat transfer of nanofluid in comparison with the base fluid. However, the addition of nanoparticles in the base fluid would also affect the other thermo-physical properties such as dynamic viscosity, density and heat capacity of the base fluid. Therefore, the addition of nanoparticles may enhance the heat transfer coefficient of nanofluid even further than the enhancement in the thermal conductivity, or sometimes it may decrease the heat transfer coefficient to values less than the heat transfer coefficient of the base fluid. The previous studies [5-7] show that the concentration of nanoparticles in the base fluid may not remain constant, and the nanoparticles may have a slip velocity relative to the base fluid. The slip of nanoparticles can transfer energy and affect the local thermo-physical properties of the nanofluid [6, 8].

Currently, there are two general approaches to analyze the convective heat transfer of nanofluids. In the first approach, the nanofluid is considered as a homogenous mixture of the nanoparticles and the base fluid [8-10]. Hence, the nanofluid is a single-phase fluid with enhanced thermo-physical properties, and hence, the conventional governing equations of momentum and energy can be utilized to analyze the flow and heat transfer of nanofluids.

In the second approach, the nanofluid may not remain homogenous and the nanoparticles may have slip velocity relative to the base fluid. Using scale analyze, Buongiorno [6] have examined the forces, which may act on the nanoparticles in the base fluid. The results show that the Brownian motion and thermophoresis are the main important forces causing the drift flux (slip velocity) of nanoparticles in the base fluid [11-18].

Using a homogeneous model of nanofluid, Bachok et al. [9] have analyzed the boundary layer flow and heat transfer of nanofluids over a flat plate. They performed a case study for the Cu, Al₂O₃ and TiO₂ nanoparticles dispersed in the water. They utilized the Maxwell model [19] for evaluation of thermal conductivity of the nanofluids. They [9] adopted the Brinkman model [20] to evaluate the viscosity of the nanofluids. As the Maxwell and Brinkman models are independent of the size of nanoparticles, the effect of the size of nanoparticles on the boundary layer was not examined in the study of Bachok et al. [9]. Bachok et al. [9] were adopted the reduced Nusselt number ($Nu_x/Re_x^{1/2} = -k_{nf} \theta'(0)/k_f$) as the important heat transfer parameter. As seen, the reduced Nusselt number is a function of the ratio of thermal conductivity of the nanofluid and the base fluid. In the previous studies [8-11, 11-18], the Reynolds number is assumed to be fixed for both of the base fluid flow and nanofluid. However, the viscosity of nanofluid is a function of nanoparticles volume fraction. Hence, a constant free stream velocity is a more practical situation for analysis of the heat transfer of nanofluids in comparison with base fluid (rather than assuming a constant Reynolds number).

Bachok et al. [5] have examined the boundary layer flow and heat transfer of nanofluids over an isothermal flat plate using a non-homogeneous model. They considered a slip velocity for nanoparticles relative to the base fluid because of the Brownian motion and thermophoresis forces. They [5] assumed that the concentration of nanoparticles is actively controlled to be constant on the surface. In the work of Bachok et al. [5], the governing equations are a function of Prandtl number, Lewis number, Brownian motion parameter and thermophoresis parameter. The reduced Nusselt number was introduced as the heat transfer parameter, and the results were reported for this parameter. However, in the non-homogenous model, the variation of reduced Nusselt number ($Nur = Re_x^{1/2} \times h_{nf} x / k_{nf}$) cannot adequately show the heat transfer enhancement of nanofluid in comparison with the base fluid. The presence of nanoparticles simultaneously affects the surface heat transfer coefficient (h_{nf}) and increases the thermal conductivity of the nanofluid (k_{nf}). Hence, the reduced Nusselt number may decrease; however, the heat transfer coefficient may increase.

In the previous works [5, 7-18], the effect of local volume fraction of nanoparticles on the thermal conductivity and viscosity of nanofluids was neglected. However, the experimental measurement of the thermo-physical properties of nanofluids shows that the thermal conductivity and viscosity of nanofluids strongly depends on the volume fraction of nanoparticles [2, 21]. Therefore, in the present study, the thermal conductivity and viscosity of nanofluid are considered as a function of local volume fraction of nanoparticles.

In the previous studies [7, 11-18], which have utilized the non-homogeneous model of nanofluids, the volume fraction of nanoparticles at the wall was assumed to be actively controlled in the concentrations higher than the concentration of the free stream, but no identification was given how the surface can actively control the volume fraction of nanoparticles. Hence, in the present study, the zero flux of nanoparticles at the plate, which is a more realistic boundary condition, is adopted. Consequently, the volume fraction of nanoparticles at the surface of the plate is evaluated using the solution of the governing equations.

In practice, the engineers need to know the convective enhancement of using nanofluids in comparison with the base fluid. However, the measurement of the thermophysical properties of nanofluids could not adequately indicate the convective heat transfer enhancement of nanofluids. For example, a scientist may synthesized a new nanofluid, using a nanopowder or a chemical

method, for heat transfer applications and then measure the thermophysical properties of the nanofluid. The measurement results typically indicate enhancement in the thermal conductivity as well as the dynamic viscosity. It is clear that the increase of the thermal conductivity enhances the convective heat transfer, but the increase of dynamic viscosity tends to slow the flow and decrease the convective heat transfer. The other thermophysical properties (such as density and heat capacity) and the mass transfer mechanism (due to Brownian motion and thermophoresis) would also affect the convective heat of nanofluids. Now the question is that does the nanofluid enhance the convective heat transfer compared to the base fluid? Thus, a general non-dimensional analysis of the convective heat transfer for nanofluids, incorporating the effective parameters, is highly demanded to reveal the real convective enhancement of nanofluids.

In the present study the geometry of the flat plate has been adopted a typical geometry for the study of the external forced convection flows. The thermal conductivity and dynamic viscosity of nanofluid are considered as a function of local volume fraction of nanoparticles. The zero particle flux from the surface is taken into account. Two non-dimensional parameters of the number of conductivity (N_c) and number of viscosity (N_v) are introduced to show the general behavior of nanofluids for augmentation of the thermal conductivity and dynamic viscosity in the presence of nanoparticles. A non-dimensional parameter, the enhancement ratio parameter, is introduced to evaluate the heat transfer enhancement of nanofluids in comparison with the base fluid.

2. MATHEMATICAL FORMULATIONS

Consider the two-dimensional incompressible and steady forced convection boundary layer flow of a nanofluid over a horizontal and isothermal flat plate. The coordinate system is chosen such that the x -axis is aligned along the plate. The schematic view of the physical model and the coordinate system are depicted in Fig. 1. Following the scale analysis reported by Buongiorno [6], the nanoparticles in the fluid are subject to the thermophoresis and Brownian motion forces. The thermophoresis tends to move the nanoparticles from hot to cold [6]. The Brownian motion tends to move the particles from high concentration areas to low concentration ones. In the present study, it is assumed that the plate is hot, and hence, the nanoparticles would move away from the plate because of the thermophoresis effect. In contrast, the Brownian motion tends to uniform the concentration of nanoparticles in the base fluid. Hence, there is a concentration boundary layer of nanoparticles over the plate. Considering hydrodynamic boundary layer, thermal boundary layer and nanoparticles concentration boundary layer, there are three distinct boundary layers over the plate. These boundary layers are depicted in the Fig. 1.

It is assumed that the plate is isothermal, and the mass flux of the nanoparticles at the plate is zero. The nanoparticles volume fraction, temperature and velocity of the free stream are denoted by values of ϕ_∞ , T_∞ and U_∞ , respectively. As mentioned, the volume fraction of nanoparticles strongly influence the thermal conductivity and dynamic viscosity of nanofluids [1, 2]. Therefore, in the present study, the thermal conductivity and dynamic viscosity of the nanofluids are assumed as a function of local volume fraction of nanoparticles.

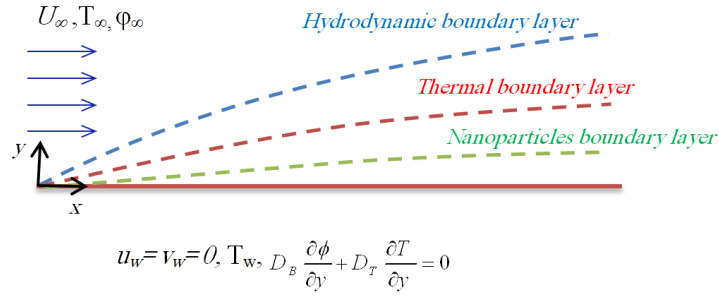


Figure 1. Physical model and coordinate system.

Following the work of Buongiorno [6], the governing equations, which are the mixture continuity equation, the mixture momentum equation, the mixture thermal energy equation and the dispersed phase continuity equation, are written as follows, respectively:

$$\nabla \cdot (V_{nf}) = 0 \tag{1}$$

$$V_{nf} \cdot \nabla V_{nf} = -\nabla P_{nf} + \nabla \cdot (\mu_{nf} \nabla V_{nf}) \tag{2}$$

$$(\rho c)_{nf} (V_{nf} \cdot \nabla T) = \nabla \cdot (k_{nf} \nabla T) - c_p j_p \cdot \nabla T \tag{3}$$

$$V_{nf} \cdot \nabla \phi = -\frac{1}{\rho_p} \nabla \cdot j_p \tag{4}$$

$$\text{where } j_p = -\rho_p D_B \nabla \phi - \rho_p D_T \frac{\nabla T}{T}.$$

The corresponding boundary conditions are as follows:

$$u_{nf} = v_{nf} = 0, \quad T = T_w, \quad D_B \frac{\partial \phi}{\partial y} + D_T \frac{\partial T}{\partial y} = 0, \quad \text{at } y = 0. \tag{5-a}$$

$$u_{nf} \rightarrow u_{nf, \infty}, \quad T \rightarrow T_\infty, \quad \phi \rightarrow \phi_\infty, \quad \text{at } y \rightarrow \infty. \tag{5-b}$$

where subscripts of ∞ and w indicate the properties outside the boundary layer and at the wall, respectively. The subscripts of P , nf and f indicate the nanoparticles, nanofluid and base fluid, respectively. It is worth noticing that the zero mass flux of nanoparticles at the surface, i.e. $D_B \frac{\partial \phi}{\partial y} + D_T \frac{\partial T}{\partial y} = 0$, in some cases (when the thermophoresis force is very strong) may lead to negative values of nanoparticles volume fraction on the surface. In this situation, the zero mass flux of nanoparticles at the surface $D_B \frac{\partial \phi}{\partial y} + D_T \frac{\partial T}{\partial y} = 0$ could be replaced by the zero volume fractions of nanoparticles at the surface. The continuity equation, Eq. (1), is satisfied by introducing the stream function (ψ):

$$u = \frac{\partial \psi}{\partial y}, \quad v = -\frac{\partial \psi}{\partial x}, \tag{6}$$

Here, in order to attain a similarity solution, the local Reynolds number, Re_x , and the similarity variable, η , are introduced as:

$$\text{Re}_x = \frac{\rho_{nf} U_{nf,\infty} x}{\mu_{nf}}, \quad (7)$$

$$\eta = \frac{y}{x} \text{Re}_x^{\frac{1}{2}}. \quad (8)$$

The dimensionless similarity quantities S , θ , and f are introduced:

$$S = \frac{\psi}{(U_{\infty} v_{nf} x)^{\frac{1}{2}}}, \quad \theta = \frac{T - T_{\infty}}{T_w - T_{\infty}}, \quad f = \frac{\phi - \phi_{\infty}}{\phi_{\infty}} \quad (9)$$

Employing the usual boundary layer approximations and invoking Eqs. (6)-(8), the governing equations of Eqs. (1)-(3) are transformed into the following set of non-linear ordinary differential equations (see Appendix A):

$$\left(\frac{\mu_{nf}(f)}{\mu_{\infty}} \right)' S'' + \frac{\mu_{nf}(f)}{\mu_{\infty}} S''' + \frac{1}{2} S S'' = 0 \quad (10)$$

$$\frac{1}{Pr_{nf}} \frac{k_{nf}(f)}{k_{\infty}} \theta'' + \frac{1}{Pr} \left(\frac{k_{nf}(f)}{k_{\infty}} \right)' \theta' + \frac{1}{2} S \theta' + N_b f' \theta' + N_t \theta'^2 = 0 \quad (11)$$

$$f'' + \frac{1}{2} Le S f' + \frac{Nt}{Nb} \theta'' = 0 \quad (12)$$

subject to the following transformed boundary conditions:

$$S(0) = 0, \quad S'(0) = 0, \quad \theta(0) = 1, \quad N_b f'(0) + N_t \theta'(0) = 0 \quad (13-a)$$

$$S'(\eta) \rightarrow 1, \quad \theta(\eta) \rightarrow 0, \quad f(\eta) \rightarrow 0, \quad \text{as } \eta \rightarrow \infty \quad (13-b)$$

where ' denote $\partial/\partial\eta$, and the non-dimensional parameters are:

$$Pr = \frac{\nu_{nf,\infty}}{\alpha_{nf,\infty}} \quad (14-a)$$

$$Nb = \frac{(\rho c)_p D_B \phi_{\infty}}{(\rho c)_{nf} \nu_{nf}} \quad (14-b)$$

$$Nt = \frac{(\rho c)_p D_T (T_w - T_{\infty})}{(\rho c)_{nf} \nu_{nf} T_{\infty}} \quad (14-c)$$

$$Le = \frac{\nu_{nf,\infty}}{D_{nf,B}} \quad (14-d)$$

where Pr , Nb , Nt and Le are Prandtl number, Brownian motion parameters, thermophoresis parameter and Lewis number, respectively. As mentioned, if the zero mass flux of nanoparticles at the surface, i.e. $N_b f'(0) + N_t \theta'(0) = 0$, leads to negative values of the volume fraction of

nanoparticles at the surface, it would be replaced by the zero volume fraction of nanoparticles ($f'(0)=-1$). The quantities of local Nusselt number (Nu_x) and local skin friction, Cf_x , are defined as:

$$Nu_x = \frac{h \cdot x}{k_{nf, \infty}} = \frac{q_w \cdot x}{k_{nf, \infty} (T_w - T_\infty)} \quad (15-a)$$

$$Cf_x = \frac{\tau_{nf, w}}{\rho_f U_\infty^2} \quad (15-b)$$

where the quantity of q_w is the wall heat flux ($-k_{nf, w} \partial T / \partial y$ at $y=0$) and τ_w is the wall skin friction ($\mu_{nf, w} \partial u / \partial y$ at $y=0$). The Nusselt number shows the non-dimensional heat transfer, and the skin friction parameter indicates the non-dimensional required pump power to maintain the fluid flowing over the plate. The mass transfer from the wall, Sherwood number, is identically zero. Using similarity variables, the local Nusselt number (Nu_x) and local skin friction are obtained as:

$$Nu_x \text{Re}_{nf, x}^{-\frac{1}{2}} = -\frac{k_{nf, w}}{k_{nf, \infty}} \theta'(0), \quad (16-a)$$

$$Cf_x \text{Re}_{nf, x}^{\frac{1}{2}} = \frac{\mu_{nf, w}}{\mu_{nf, \infty}} S''(0) \quad (16-b)$$

where $Nu_x \times \text{Re}_x^{-1/2}$ is the reduced Nusselt number, *Nur*. Buongiorno *et al.* [22] and Venerus *et al.* [23], using benchmark experimental tests, demonstrated that the thermal conductivity and dynamic viscosity of nanofluids are a linear function of volume fraction of nanoparticles. Therefore, following the experimental results, the local thermal conductivity and dynamic viscosity of nanofluids are evaluated using the following relations:

$$\frac{k_{nf}}{k_{nf, \infty}} = 1 + Nc \frac{(\phi - \phi_\infty)}{\phi_\infty} \quad (17a)$$

$$\frac{\mu_{nf}}{\mu_{nf, \infty}} = 1 + Nv \frac{(\phi - \phi_\infty)}{\phi_\infty} \quad (17b)$$

where Nc and Nv are non-dimensional parameters which are a function of type of the base, shape of nanoparticles, size of nanoparticles, type of nanoparticles, the working temperature, and synthesized method of nanofluid [3]. The parameters of Nc (number of conductivity) and Nv (number of viscosity) can be evaluated using curve fitting on the reported experimental data. It is clear that the local volume fractions of nanoparticles can be vary in the range of zero volume fraction of nanoparticles at the surface ($\phi_w=0$ or $f'(0)=-1$) and free stream volume fraction of nanoparticles on the surface ($\phi_w = \phi_\infty$ or $f'(0)=0$). Hence, substituting these two extreme limits for the concentration of nanoparticles in Eqs. 17a and 17b, results in $Nc=1-k_{bf}/k_{nf, \infty}$ and $Nv=1-\mu_{bf}/\mu_{nf, \infty}$. The literature review shows that the previous studies have commonly utilized the Maxwell and Brinkman relations for evaluating the thermal conductivity and the dynamic viscosity of nanofluids, respectively [8, 9]. Hence, here, the validity of, Eqs. (17-a) and (17-b), is checked against the Maxwell and Brinkman relations for Al_2O_3 - water nanofluids in the Fig. 2. This figure depicts $k_{nf}/k_{nf, \infty}$ and $\mu_{nf}/\mu_{nf, \infty}$ as a function of local volume fraction of nanoparticles, evaluated using Eqs. (17a) and (17b) as well as the analytical relations of Maxwell [2, 19] and Brinkman models [2, 20]. As seen, there is an excellent agreement between the results of the analytic models and Eqs. (17a) and (17b). Therefore, Eqs. (17-a) and (17-b) are utilized in computations

to evaluate the effect of the local concentration of nanoparticles on the thermal conductivity and dynamic viscosity of nanofluids. It should be noticed that further experimental results and theoretical models can also be modeled by adjusting the non-dimensional values of Nc and Nv . Indeed, these parameters show the thermophysical properties of nanofluids in a general form.

Hence, in the following text the results are reported for various values of Nc and Nv parameters.

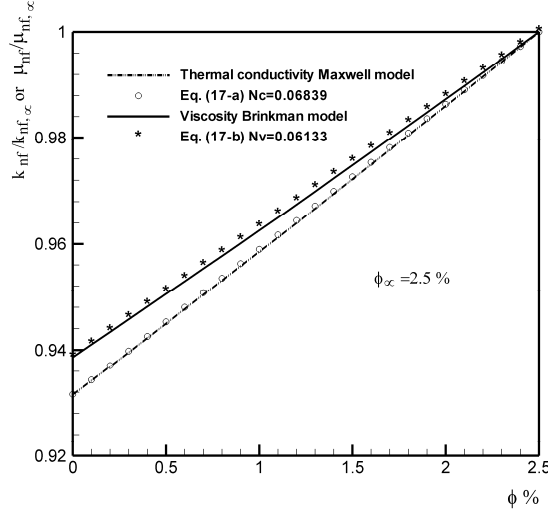


Figure 2. Comparison between the evaluated values of local thermal conductivity and local viscosity of nanofluid as a function of local volume fraction of nanoparticles

Here, using Eqs. (17-a) and (17-b), the reduced Nusselt number and the reduced skin friction are written as:

$$Nur = -(1 + Nc f(0)) \theta'_{nf}(0), \quad (18-a)$$

$$C_f Re_{\infty,x}^{\frac{1}{2}} = (1 + Nv f(0)) S''(0) \quad (18-b)$$

In order to examine the heat transfer enhancement achieved by using nanoparticles, compared to the base fluid, the enhancement ratio parameter is introduced as:

$$\frac{h_{drift-flux}}{h_{bf}} = (1 - Nv)^{\frac{1}{2}} \frac{1 + Nc f(0)}{1 - Nc} \frac{\theta'_{nf}(0)}{\theta'_{bf}(0)} \left(\frac{\rho_{nf}}{\rho_{bf}} \right)^{\frac{1}{2}} \quad (19)$$

The enhancement ratio shows the ratio of the convective heat transfer onanofluids to the convective heat transfer of the base fluid. The presence of nanoparticles in the base fluid influences the viscosity and other thermo-physical properties of the host fluid. As the Reynolds number is a function of the fluid properties, the Reynolds numbers of the nanofluid and the base fluid are not identical. In addition, the presence of nanoparticles increases the thermal conductivity of the base fluid. Therefore, the reduced Nusselt number of nanofluid ($Nur_{nf} = Re_{nf}^{-1/2} \times h_{nf,x}/k_{nf}$) may decrease (because of the increase of the thermal conductivity); however, the heat transfer coefficient, h , may increase. In addition, the presence of nanoparticles increases the dynamic viscosity of the base fluid,

and consequently, it affects the Reynolds number. Hence, the Reynolds number is a decreasing function of volume fraction of nanoparticles. The decrease of the Reynolds number, consequently, tends to reduce the heat transfer coefficient, h_{nf} . Therefore, the variation of reduced Nusselt number cannot adequately show the enhancement of using nanoparticles. In contrast, but the effect of presence of nanoparticles on the heat transfer enactment can be adequately seen in the enhancement ratio parameter.

As the most of nanofluids are dilute mixture of nanoparticles, dispersed in a base fluid, the density of the nanofluid is about the density of the base fluid. For example, $(\rho_{nf}/\rho_{bf})^{1/2}$ is obtained as 0.99 for a practical case with 2.5% volume fraction of Al_2O_3 nanoparticles dispersed in the water. The value of $(\rho_{nf}/\rho_{bf})^{1/2}$ is about unit. Hence, the term $(\rho_{nf}/\rho_{bf})^{1/2}$ is assumed as unity in the following text for convenience.

Finally, the enhancement ratio, which compares the convective heat transfer coefficients of the non-homogeneous model ($h_{drift-flux}$) and the homogeneous model (h_{hom}), is introduced as follow:

$$\frac{h_{drift-flux}}{h_{hom}} = (1 + Nc.f(0)) \frac{\theta'_{drift-flux}(0)}{\theta'_{hom}(0)} \quad (20)$$

which compares the evaluated enhancement using the non-homogeneous model ($h_{drift-flux}$) and the homogeneous model (h_{hom}).

3. NUMERICAL METHOD

Eqs. (17-a) and (17-b) and their derivatives are substituted in the governing equations, i.e. Eqs. (10) and (11). The Prandtl number for the nanofluids can be evaluated using $Pr_{nf} = Pr_{bf} \times (c_{nf}/c_{bf}) \times (1 - Nc)/(1 - Nv)$. Later, the governing equations, Eq. (10)-(12), including the variable thermal conductivity and variable dynamic viscosity (i.e. Eqs. (17-a) and (17-b)) subject to the boundary conditions, Eqs. (13-a) and (12-b), are numerically solved using a finite difference solver that implements the 3-stage Lobatto IIIa formula with a collocation formula to uniform the error in the domain of the solution associated with an automatic mesh adaptation. The solver is the same as the work Shampine et al. [24]. A maximum relative error of 10^{-8} is used as the stopping criteria for the iterations. The large value of $\eta_{\infty} = 10$ is adopted as the finite value of infinity for all calculations. Using $\eta_{\infty} = 10$, the results show that the boundary layer profiles asymptotically tend to zero and any further increase of η_{∞} does not change the solution. In a case in which $Nv = Nc = Nb = Nt = 0$ and $c_{nf}/c_{bf} = 1$, the present study reduces to the boundary layer heat transfer of a conventional pure fluid. In this case, the values of $\theta_{bf}'(0)$ are compared with the results reported by Lloyd and Sparrow [25] and Wilks [26]. When $Pr_{bf} = 10$ and $Pr_{bf} = 100$, the values of $\theta_{bf}'(0)$ are obtained as -0.72814 and -1.57183, respectively. Lloyd and Sparrow [25] as well as Wilks [26] obtained the values of $\theta'(0) = -0.7281$ and $\theta'(0) = -1.572$ for $Pr_{bf} = 10$ and $Pr_{bf} = 100$, respectively. Moreover, we calculated the value of $S''(0)$ as 0.33206 where Ishak *et al.* [27] reported $S''(0) = 0.3321$. It is worth mentioning that in the case of $Pr_{bf} = 7.0$ the value of $\theta_{bf}'(0)$ is computed as -0.64592.

The values of $S_{nf}''(0)/S_{bf}''(0)$, $\theta_{nf}'(0)/\theta_{bf}'(0)$, $f(0)$ are brought in Tables 1-3 for a practical combination of non-dimensional parameters. The results of Tables 1-3 are computed using the finite difference code. The values of $f'(0)$ can be directly evaluated using the boundary condition of Eq. (16-a) (i.e. $f'(0) = -Nt.\theta'(0)/Nb$). Tables 1-3 provides all of the required initial conditions for solving Eqs. (10)-(12) by Runge-Kutta-Fehlberg method. Hence, using the results of Tables 1-3, Eqs. (10)-(12) were also solved utilizing the Runge-Kutta-Fehlberg method with variable size step and error control. The implementation of the Runge-Kutta-Fehlberg is the same as the

Appendix D.4 in the book by Curtis [28]. The maximum truncation error was fixed as 1×10^{-10} . Using Runge-Kutta-Fehlberg, the average number of steps was about 24000 steps. The results of the Runge-Kutta-Fehlberg method show that the boundary conditions are satisfied correctly. In addition, a very good agreement between the results of finite difference solver and the Runge-Kutta-Fehlberg is observed. It is worth noticing that the practical value of Lewis number is very high; hence, the thickness of the concentration boundary layer is very low in comparison with the thickness of the momentum and thermal boundary layers. Therefore, obtaining an accurate solution requires good initial guesses or using continuation methods. Hence, the results of Tables 1-3 can also be utilized as the initial guesses for future studies.

4. RESULTS AND DISCUSSION

In order to examine the effect of non-dimensional parameters on the boundary layer heat and mass transfer of nanofluids, the practical range of non-dimensional parameters should be discussed. The Brownian diffusion coefficient, D_B , as well as thermophoresis coefficient, D_T , ranges from 10^{-10} to 10^{-12} m²/s for the water base nanofluids at room temperature with nanoparticles of 100 nm diameters [6]. Assuming the conventional range of thermo-physical properties at room temperature, it is found that Nb and Nt are very small and in the range of 10^{-8} to 10^{-4} . The Lewis number is very high in the range of 10^{+3} to 10^{+5} . The parameters of variable thermal conductivity and variable viscosity conventionally are in the range of 0 to 0.2. The ratio of c_{nf}/c_{bf} is calculated for selected volume fractions of Al₂O₃ nanoparticles in the water. It is found that $c_{nf}/c_{bf}=1.0$ at (0% Vol. Al₂O₃), $c_{nf}/c_{bf}=0.98$ (at 2.5% Vol. Al₂O₃) and $c_{nf}/c_{bf}=0.96$ (at 5% Vol. Al₂O₃). Hence, c_{nf}/c_{bf} is assumed to be fixed as 0.98 for convenience in the following text.

The governing equations are solved for a typical case when $Nb=Nt=10^{-6}$, $Le=10^{+4}$, $Pr_{bf}=7.0$ and $Nc=Nv=0.1$. The results are plotted in the Fig. 3. This figure depicts the non-dimensional profiles of velocity, temperature, and concentration of nanofluids over a flat plate. The concentration profile was negative; hence, it was multiplied by -10 and then plotted in the Fig. 3 for convenience. As seen, all of the profiles asymptotically tend to the boundary conditions as η increases. It is clear that the thickness of the concentration boundary layer is much lower than that of the hydrodynamic and thermal boundary layers. This is in good agreement with the physics of the concentration boundary layer as the Lewis number is very high for nanofluids. The Lewis number shows the ratio of cinematic viscosity of the nanofluid to the Brownian diffusion coefficient. As the Brownian diffusion coefficient (D_B) is very small, the Lewis number is very large. Hence, it is expected that the thickness of the concentration boundary layer to be much lower than that of the hydrodynamic boundary layer. Moreover, the Prandtl number for nanofluids is comparatively high ($Pr_{bf}>1$), and hence, the thickness of the hydrodynamic boundary layer is higher than the thickness of the thermal boundary layer as seen in Fig. 3.

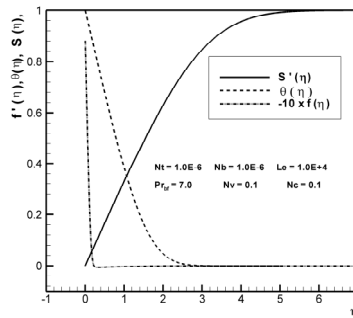


Figure 3. The velocity, temperature and concentration profiles for a typical case.

The governing differential equations, Eqs. (10)-(12), are numerically solved for different combinations of non-dimensional parameters. It is found that the variation of thermophoresis parameter, Brownian motion parameter, and Lewis number does not show significant effect on the velocity and temperature profiles. Indeed, the Brownian motion and thermophoresis parameters are very small, and hence, the direct effect of variation of these parameters on the energy equation can be neglected. However, in the equation of nanoparticles conservation, the ratio of the thermophoresis parameter to Brownian motion parameter (i.e. Nt/Nb) is not negligible and may induce significant effects on the concentration boundary layer of nanoparticles. The concentration boundary layer consequently induces indirect effects on the hydrodynamic and thermal boundary layer through the variation of the thermo-physical properties.

It is also found that the effect of the variable thermal conductivity parameter (Nv) as well as the variable viscosity parameter (Nc) on the boundary layer profiles (i.e. hydrodynamic, thermal and concentration profiles) is comparatively negligible. However, the effect of these parameters, Nc and Nv , on the surface skin friction and surface heat transfer is completely significant. This is because of the impact of these parameters on the thermo-physical properties. As mentioned, the effect of non-dimensional parameters, i.e. Nb , Nt , Le , Nc and Nv , on the non-dimensional velocity and temperature profiles is comparatively negligible. Thus, only the effect of non-dimensional parameters on the concentration profiles is plotted in the Figs. 4-5.

Fig. 4(a) depicts the effect of Brownian motion parameter on the concentration profiles. This figure illustrates that an increase of Brownian motion parameter (considering the negative sign) would increase the values of the concentration profiles in the vicinity of the plate. The zero values of concentration profiles, $f(\eta) \rightarrow 0$, indicates that the local volume fraction of nanoparticles is about the free stream volume fraction. $f(\eta) \rightarrow -1$ indicates that the local volume fraction of nanoparticles tends to zero. The positive values of the concentration profiles in the vicinity of the plate indicate that the volume fraction of nanoparticles is higher than the concentration of the free stream flow. As seen, there are two branches of behavior for concentration profiles. The first branch of behavior is when the Brownian motion parameter is very low (in this case between 10^{-9} to 10^{-8}). In this case, the volume fraction of nanoparticles at the surface would remain zero (because the negative volume fraction of nanoparticles is not allowed); this is where the $f(0) = -1$. Therefore, in the first branch of the behavior, the thermophoresis effect is the dominant effect and tends to strongly move the nanoparticles away from the surface. Consequently, the nanoparticles which are swept from the surface would be gathered in the vicinity of the plate (this is where the concentration of nanoparticles is higher than the concentration of the free stream $f(0) > 0$). Later, the Brownian motion effect would tend to uniform the nanoparticles toward the edge of the concentration boundary layer smoothly. The augmentation of the Brownian motion parameter tends to reduce the peak of the high concentration region. In the second branch of behavior, the Brownian motion forces are comparable with the thermophoresis forces. In these cases, the volume fractions of nanoparticles at the surface are less than the free stream volume fraction; however, they are not zero anymore. The increase of Brownian motion parameter would increase the concentration of nanoparticles up to the concentration of free stream. Therefore, for high values of Brownian motion parameter, the nanoparticles in the entire of the boundary layer are almost uniform. As seen, in the second branch of the behavior (i.e. $f(0) > -1$), the variation of Brownian motion parameter does not affect the thickness of the boundary layer. Indeed, the concentration of nanoparticles at the plate would be adjusted by the balance between the Brownian motion force and the thermophoresis force. However, in the first branch of behavior, in which the volume fraction of nanoparticles is zero, the Brownian motion and thermophoresis forces would be balanced in the boundary layer (not at the surface). Therefore, in this case (i.e. $f(0) > -1$) the thickness of the concentration boundary layer is significantly affected by the Brownian motion parameter (i.e. an increase of Brownian motion parameter would decrease the boundary layer thickness). Fig. 4(b) depicts the effect of the thermophoresis parameter on the concentration profiles. As seen, the concentration of nanoparticles at the surface tends to zero for

high values of the thermophoresis parameters. However, for comparatively low values of the thermophoresis parameter, the concentration of nanoparticles at the surface is lower than the concentration of the free stream. For very low values of the thermophoresis parameter ($Nt = 10^{-9}$), the boundary layer of nanoparticles almost vanished. The results of this figure are in very good agreement with the results of Fig. 4(a).

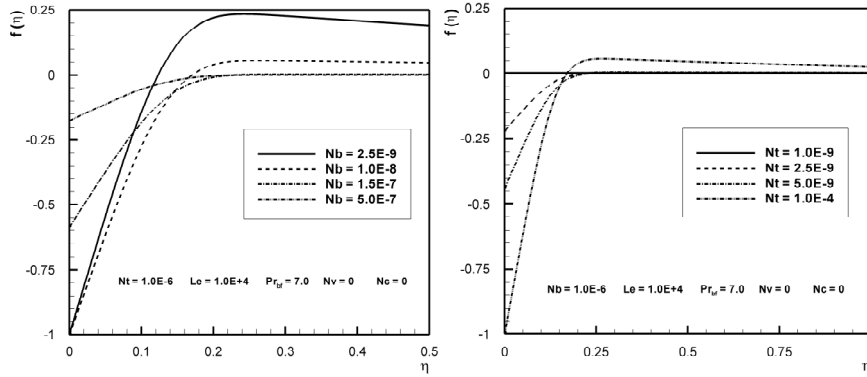


Figure 4. The concentration profiles for selected values of (a) Brownian motion and (b) of thermophoresis parameters.

Figs. 5(a) and 5(b) show the effect of Lewis (Le) and Prandtl (Pr) numbers on the concentration profiles, respectively. As mentioned, a raise in the Lewis number would decrease the thickness of the concentration boundary layer. The Prandtl number comparatively shows the ratio of the thickness of the hydrodynamic boundary layer to the thermal boundary layer. The thickness of the non-dimensional hydrodynamic boundary layer is almost fixed. Hence, an increase of Prandtl number would reduce the thickness of the thermal boundary layer. The thinner are the thermal boundary layers, the higher are the temperature gradients near the surface. Consequently, as the temperature gradient increases the thermophoresis force increases. An increase of the thermophoresis force would decrease the concentration of nanoparticles. Therefore, it would be expected that augmentation of Prandtl number reduce the concentration of nanoparticles in the vicinity of the plate (As seen in Fig. 5(b)).

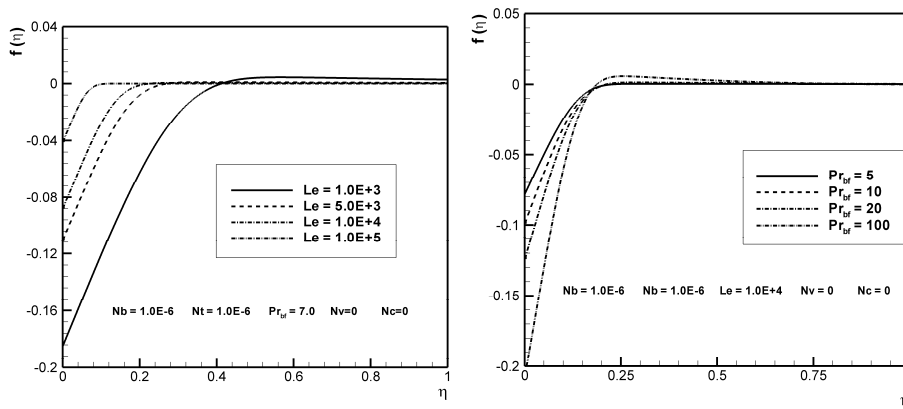


Figure 5: The concentration profiles for selected values of (a) Lewis and (b) Prandtl Numbers.

It is found that variations of the number of conductivity (Nc) and the number of viscosity (Nv) parameters induce a very slight effect on the boundary layer profiles. Hence, the variation of boundary layer profiles as a function of these parameters was not depicted in figures. However,

the results indicate that an increase of Nc would slightly decrease the temperature profiles in the boundary layer. An increase of Nv would slightly increase the temperature profiles and decrease the velocity profiles. Therefore, as Nc increases, $\theta'(0)$ slightly increases. Moreover, as the Nv increases, $S''(0)$ slightly increases and $\theta'(0)$ decreases.

Fig. 6 shows the variation of $f(0)$ as a function of Brownian motion parameter for selected values of the thermophoresis parameter and Lewis number when the variable thermal conductivity (Nc) and variable viscosity (Nv) parameters are zero. In this figure, the curves with diamond symbols depict the results for $Le=10^{+3}$. As the Brownian motion parameter is a very small value, this parameter is plotted in the logarithmic scale. An augmentation of the Brownian motion parameter would reduce the magnitude of $-f(0)$. In contrast, an increase of thermophoresis parameters would increase the magnitude of $-f(0)$. It is clear that $f(0)$ could reach to the constant value of -1 for high values of thermophoresis parameter and low values of Brownian motion parameter. The constant value of -1 is the physical limit of non-dimensional concentration at the plate which shows the zero volume fractions of nanoparticles at the surface. The concentrations lower than -1 shows negative volume fractions of nanoparticles which physically is not possible. As the Lewis number increases, the magnitude of $-f(0)$ decreases (i.e. the volume fraction of nanoparticles at the plate increases). As seen, the results of this figure are in good agreement with the results of previous figures.

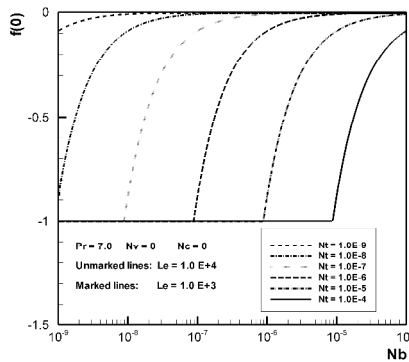


Figure 6: The non-dimensional concentration at the plate ($f(0)$) as a function of Nb for selected values of thermophoresis parameter when $Le = 1.0E+3$ and $Le = 1.0E+4$.

The variation of non-dimensional values of the surface skin friction, $S_{nf}''(0)/S_{bf}''(0)$, temperature gradient, $\theta_{nf}'(0)/\theta_{bf}'(0)$ and surface concentration are shown in Tables 1-3 respectively, for selected values of the non-dimensional parameters (i.e. Nb , Nt , Le , Pr , Nc and Nv). The values of non-dimensional parameters are selected in agreement with the practical range of these parameters. It is worth noticing that the value of $S_{bf}''(0)$ is fixed as 0.33206 for the base fluid. The non-dimensional temperature gradient of the base fluid at the surface, $\theta_{bf}'(0)$, is only a function of Prandtl number. The corresponding values of $\theta_{bf}'(0)$ for $Pr_{bf}=7.0$ and $Pr_{bf}=100$ were mentioned in the previous section. Tables 1 and 2 show that the increase of the thermal conductivity parameter (Nc) would decrease the magnitude of $-f(0)$ as well as $\theta_{nf}'(0)/\theta_{bf}'(0)$ in most cases. Hence, the higher Nc , the higher is nanoparticles volume fraction at the plate. In fact, the increase of Nc , which increases the volume fraction of nanoparticles in the vicinity of the plate, would increase the overall thermal conductivity of the nanofluid near the surface. As the thermal conductivity increases, the temperature gradient decreases. Consequently, a decrease of temperature gradient would reduce the thermophoresis force, which tends to move the nanoparticles away from the plate; hence the volume fraction of nanoparticles in the vicinity of the plate would increase. Hence, as seen, an increase of Nv , increases $\theta_{nf}'(0)/\theta_{bf}'(0)$, $S_{nf}''(0)/S_{bf}''(0)$ and the magnitude of $-f(0)$ in most cases. The augmentation of Nv reduces the local viscosity of the nanofluid in the vicinity of the plate (where the volume fraction of nanoparticles is lower than the volume fraction

of the free stream). Table 3 depicts that the variation of Nc does not show any effect on the $S_{nf}''(0)/S_{bf}''(0)$ when $Nv=0$. Indeed, when $Nv=0$, Eq. (12) is independent of Nc . However, when $Nv=0.1$, a raise of Nc would very slightly decrease $S_{nf}''(0)/S_{bf}''(0)$. This effect on the $S_{nf}''(0)/S_{bf}''(0)$ originates from the indirect effect of Nc on the concentration profiles. However, the effect of variation of Nc on the $S_{nf}''(0)/S_{bf}''(0)$ is comparatively negligible. It is evident that an augmentation of Nv would decrease the viscosity of the nanofluid in the vicinity of the plate (where the volume fraction of nanoparticles is lower than the volume fraction of free stream).

Table 1. The non-dimensional velocity gradient at the surface $S_{nf}''(0)/S_{bf}''(0)$

<i>Le</i>	<i>Nb</i>	<i>Nt</i>	<i>Pr_{bf}</i> =7.0				<i>Pr_{bf}</i> =100			
			<i>Nv</i> =0.0		<i>Nv</i> =0.1		<i>Nv</i> =0.0		<i>Nv</i> =0.1	
			<i>Nc</i> =0.0	<i>Nc</i> =0.1	<i>Nc</i> =0.0	<i>Nc</i> =0.1	<i>Nc</i> =0.0	<i>Nc</i> =0.1	<i>Nc</i> =0.0	<i>Nc</i> =0.1
10^{+3}	10^{-5}	10^{-5}	1.00000	1.00000	1.01926	1.01874	1.00000	1.00000	1.04290	1.04211
		10^{-6}	1.00000	1.00000	1.00190	1.00184	1.00000	1.00000	1.00415	1.00404
		10^{-7}	1.00000	1.00000	1.00019	1.00018	1.00000	1.00000	1.00041	1.00040
	10^{-6}	10^{-5}	1.00000	1.00000	1.11121	1.11122	1.00000	1.00000	1.11297	1.11295
		10^{-6}	1.00000	1.00000	1.01926	1.01874	1.00000	1.00000	1.04291	1.04212
		10^{-7}	1.00000	1.00000	1.00190	1.00184	1.00000	1.00000	1.00415	1.00404
	10^{-7}	10^{-5}	1.00000	1.00000	1.11904	1.11883	1.00000	1.00000	1.13065	1.12990
		10^{-6}	1.00000	1.00000	1.11121	1.11122	1.00000	1.00000	1.11297	1.11295
		10^{-7}	1.00000	1.00000	1.01926	1.01874	1.00000	1.00000	1.04291	1.04212
10^{+4}	10^{-5}	10^{-5}	1.00000	1.00000	1.00910	1.00881	1.00000	1.00000	1.02168	1.02112
		10^{-6}	1.00000	1.00000	1.00090	1.00087	1.00000	1.00000	1.00213	1.00207
		10^{-7}	1.00000	1.00000	1.00009	1.00009	1.00000	1.00000	1.00021	1.00021
	10^{-6}	10^{-5}	1.00000	1.00000	1.09733	1.09736	1.00000	1.00000	1.11124	1.11124
		10^{-6}	1.00000	1.00000	1.00910	1.00881	1.00000	1.00000	1.02169	1.02112
		10^{-7}	1.00000	1.00000	1.00090	1.00087	1.00000	1.00000	1.00213	1.00207
	10^{-7}	10^{-5}	1.00000	1.00000	1.11186	1.11186	1.00000	1.00000	1.11386	1.11379
		10^{-6}	1.00000	1.00000	1.09733	1.09736	1.00000	1.00000	1.11124	1.11124
		10^{-7}	1.00000	1.00000	1.09733	1.09736	1.00000	1.00000	1.11124	1.11124

Table 2. The non-dimensional temperature gradient on the plate $\theta_{nf}'(0)/\theta_{bf}'(0)$

<i>Le</i>	<i>Nb</i>	<i>Nt</i>	<i>Pr</i> =7.0				<i>Pr</i> =100			
			<i>Nv</i> =0.0		<i>Nv</i> =0.1		<i>Nv</i> =0.0		<i>Nv</i> =0.1	
			<i>Nc</i> =0.0	<i>Nc</i> =0.1						
10^{+3}	10^{-5}	10^{-5}	0.99320	0.97445	1.03069	1.01165	0.99311	0.99082	1.03517	1.03318
		10^{-6}	0.99322	0.96017	1.02921	0.99503	0.99327	0.96203	1.02944	0.99711
		10^{-7}	0.99323	0.95877	1.02907	0.99341	0.99328	0.95928	1.02887	0.99367
	10^{-6}	10^{-5}	0.99320	1.05622	1.03772	1.10296	0.99290	1.05987	1.03857	1.10819
		10^{-6}	0.99322	0.97447	1.03072	1.01167	0.99327	0.99097	1.03535	1.03334
		10^{-7}	0.99323	0.96017	1.02922	0.99503	0.99328	0.96205	1.02946	0.99713
	10^{-7}	10^{-5}	0.99319	1.07803	1.02949	1.11592	0.99283	1.21493	0.97653	1.19653
		10^{-6}	0.99322	1.05625	1.03775	1.10299	0.99325	1.06022	1.03896	1.10859
		10^{-7}	0.99323	0.97447	1.03072	1.01167	0.99328	0.99098	1.03536	1.03336
10^{+4}	10^{-5}	10^{-5}	0.99320	0.96640	1.02944	1.00193	0.99298	0.97635	1.03053	1.01367
		10^{-6}	0.99322	0.95939	1.02909	0.99409	0.99325	0.96068	1.02898	0.99528
		10^{-7}	0.99323	0.95869	1.02905	0.99331	0.99328	0.95915	1.02883	0.99348
	10^{-6}	10^{-5}	0.99320	1.04596	1.03332	1.08967	0.99289	1.05574	1.03764	1.10264
		10^{-6}	0.99322	0.96642	1.02947	1.00196	0.99325	0.97660	1.03084	1.01396
		10^{-7}	0.99323	0.95939	1.02909	0.99409	0.99328	0.96070	1.02901	0.99531
	10^{-7}	10^{-5}	0.99319	1.06319	1.03277	1.10467	0.99281	1.08489	1.02413	1.11771
		10^{-6}	0.99322	1.04598	1.03335	1.08970	0.99324	1.05609	1.03805	1.10305
		10^{-7}	0.99323	0.96642	1.02947	1.00196	0.99328	0.97663	1.03087	1.01399

Table 3. The non-dimensional concentration profiles on the plate- $f(0)$

Le	Nb	Nt	$Pr=7.0$				$Pr=100$			
			$Nv=0.0$		$Nv=0.1$		$Nv=0.0$		$Nv=0.1$	
			$Nc=0.0$	$Nc=0.1$	$Nc=0$	$Nc=0.1$	$Nc=0$	$Nc=0.1$	$Nc=0$	$Nc=0.1$
10^{+3}	10^5	10^{-5}	0.18381	0.17882	0.18948	0.18440	0.40233	0.39507	0.41180	0.40452
		10^{-6}	0.01838	0.01778	0.01900	0.01839	0.04024	0.03917	0.04134	0.04026
		10^{-7}	0.00184	0.00178	0.00190	0.00184	0.00402	0.00391	0.00414	0.00402
	10^6	10^{-5}	1.00000	1.00000	1.00000	1.00000	1.00000	1.00000	1.00000	1.00000
		10^{-6}	0.18381	0.17882	0.18949	0.18441	0.40238	0.39511	0.41184	0.40457
		10^{-7}	0.01838	0.01778	0.01900	0.01839	0.04024	0.03917	0.04134	0.04026
	10^7	10^{-5}	1.00000	1.00000	1.00000	1.00000	1.00000	1.00000	1.00000	1.00000
		10^{-6}	1.00000	1.00000	1.00000	1.00000	1.00000	1.00000	1.00000	1.00000
		10^{-7}	0.18381	0.17882	0.18949	0.18441	0.40238	0.39512	0.41185	0.40457
10^{+4}	10^5	10^{-5}	0.08729	0.08456	0.09023	0.08743	0.20612	0.20078	0.21228	0.20685
		10^{-6}	0.00873	0.00843	0.00904	0.00873	0.02062	0.01996	0.02130	0.02062
		10^{-7}	0.00087	0.00084	0.00090	0.00087	0.00206	0.00200	0.00213	0.00206
	10^6	10^{-5}	0.87286	0.87257	0.88750	0.88773	1.00000	1.00000	1.00000	1.00000
		10^{-6}	0.08729	0.08456	0.09023	0.08743	0.20616	0.20083	0.21233	0.20690
		10^{-7}	0.00873	0.00843	0.00904	0.00873	0.02062	0.01996	0.02130	0.02062
	10^7	10^{-5}	1.00000	1.00000	1.00000	1.00000	1.00000	1.00000	1.00000	1.00000
		10^{-6}	0.87288	0.87259	0.88753	0.88775	1.00000	1.00000	1.00000	1.00000
		10^{-7}	0.08729	0.08456	0.09023	0.08743	0.20617	0.20083	0.21234	0.20690

Table 4. The values of $S''(0)$ and $\theta'(0)$ for homogenous model of nanofluid $Pr_{nf}=0.98 \times Pr_{bf} \times (1-Nc)/(1-Nv)$

	$Pr_{bf}=7.0$				$Pr_{bf}=100$			
	$Nv=0.0$		$Nv=0.1$		$Nv=0.0$		$Nv=0.1$	
	$Nc=0.0$	$Nc=0.1$	$Nc=0$	$Nc=0.1$	$Nc=0$	$Nc=0.1$	$Nc=0$	$Nc=0.1$
$S''(0)$	0.332057	0.332057	0.332057	0.332057	0.332057	0.332057	1.617118	1.561275
$\theta'(0)$	0.641547	0.619192	0.664686	0.641547	1.561275	1.507357	0.332057	0.332057

It is clear that an increase of the thermophoresis parameter (Nt) or decrease of the Brownian motion parameter (Nb) would increase the magnitude of $-f(0)$ at the surface, which results in decrease of the volume fraction of nanoparticles in the vicinity of the plate. However, for zero values of Nc and Nv (i.e. model of constant thermo physical properties), the variation of Nb and Nt induce a very slight effect of on the $\theta_{nf}'(0)/\theta_{bf}'(0)$, and hence, the effect of Nb as well as Nt on the non-dimensional temperature gradient at the wall can be neglected in the case of $Nv=Nc=0$. This slight variation of $\theta_{nf}'(0)/\theta_{bf}'(0)$ is because of the small contribution of migration of nanoparticles (i.e. the terms of thermophoresis and Brownian motion) in the energy equation. However, for conventional values of variable thermal conductivity and viscosity parameters (i.e. $Nc=Nv=0.1$), the increase of Nt would increase $\theta_{nf}'(0)/\theta_{bf}'(0)$. By contrast, an increase of Nb would decrease $\theta_{nf}'(0)/\theta_{bf}'(0)$. In this case (i.e. $Nc=Nv=0.1$), the variation of thermo-physical properties because of the variation of volume fraction of nanoparticles ($-f(0)$) is the dominant effect in the vicinity of the plate.

The variable viscosity parameter induces a significant effect on the non-dimensional surface skin friction, $S_{nf}''(0)/S_{bf}''(0)$. However, the effect of Nc on the $S_{nf}''(0)/S_{bf}''(0)$ is negligible. This is because of the fact that Nv directly affects the viscosity of nanofluid near the surface, but Nc first affects the concentration profiles, and consequently, the concentration profiles affect the momentum boundary layer through the variation of dynamic viscosity of the nanofluid. An increase of Nt or decrease of Nb would increase the non-dimensional surface skin friction, $S_{nf}''(0)/S_{bf}''(0)$.

The effect of Lewis and Prandtl numbers on the magnitude of non-dimensional temperature gradient, $\theta_{nf}'(0)/\theta_{bf}'(0)$, and surface friction, $S_{nf}''(0)/S_{bf}''(0)$, is very slight. However, an augmentation of Prandtl number would raise the magnitude of $-f(0)$, which reduces the volume fraction of nanoparticles at the surface. In contrast, a raise of Lewis number would reduce the magnitude of $-f(0)$. An increase of Prandtl number would decrease the thickness of thermal boundary layer, and consequently, the temperature near the plate would increase; hence, the thermophoresis force will be boosted and in results the volume fraction of nanoparticles would decrease (i.e. the magnitude of $-f(0)$ would increase). In contrast, the augmentation of Lewis number would reduce the thickness of the concentration boundary layer, which leads to increase of Brownian force and consequently increase of the volume fraction of nanoparticles (i.e. the magnitude of $-f(0)$ would decrease).

The values of the enhancement ratio of the nanofluid to the base fluid can be easily obtained using Eq. (19) and the results of Tables 1 and 2. The maximum value of enhancement ratio ($h_{drift-flux}/h_{bf}$) is obtained as 1.22 for the case of $Nb=10^{-7}$, $Nt=10^{-5}$, $Pr_{bf}=100$, $Le=10^{+3}$, $Nv=0$ and $Nc=0.1$; the minimum value of the enhancement ratio is obtained as 0.926 for the case of $Nb=10^{-7}$, $Nt=10^{-5}$, $Pr=100$, $Le=10^{+3}$, $Nv=0.1$ and $Nc=0$. Therefore, it can be concluded that using nanoparticles does not always enhance the heat transfer rate. In some cases, using nanoparticles would increase the heat transfer about 22%; however, in some other cases, the heat transfer may even decrease about -7%. However, for a typical case (i.e. $Nc=0.1$ and $Nv=0.1$), the values of enhancement ratio are calculated between 1.045 and 1.135.

The enhancement ratio of non-homogenous (drift-flux) model to the homogenous model is also calculated for the results of Tables 1 and 2. It is found that the maximum value of the enhancement ratio ($h_{drift-flux}/h_{hom}$) is 1.140 for the case of $Nb=10^{-7}$, $Nt=10^{-5}$, $Pr=100$, $Le=10^{+3}$, $Nv=0.1$ and $Nc=0.1$; the minimum value of the enhancement ratio ($h_{drift-flux}/h_{hom}$) is obtained as 0.949 for the case of $Nb=10^{-7}$, $Nt=10^{-5}$, $Pr=100$, $Le=10^{+3}$, $Nv=0.1$ and $Nc=0.1$. Therefore, the homogeneous model may significantly underestimate the enhancement of nanofluids (about 14%) in comparison with the non-homogenous (drift-flux) model. However, in some cases, the homogeneous model may also overestimate the heat transfer of nanofluids about (5%). These results demonstrate that the concentration boundary layer significantly affects the forced convection heat transfer of nanofluids.

5. CONCLUSION

A drift flux model was utilized to examine the effect of the local concentration of nanoparticles on the boundary layer heat and mass transfer of nanofluids. The volume fraction of nanoparticles at the surface was evaluated using the zero flux of nanoparticles at the surface. The effect of local volume fraction of nanoparticles on the thermal conductivity and viscosity of nanofluids is taken into account. Considering an arbitrary function of thermal conductivity and viscosity for nanofluids, the governing partial differential equations were reduced to a set of highly nonlinear ordinary differential equations by means of similarity variables. Then, the thermal conductivity parameter (Nc) and the dynamic viscosity parameter (Nv) were introduced to evaluate the local variation of thermal conductivity and dynamic viscosity of the nanofluid. The governing equations were numerically solved for different values of non-dimensional parameters. The main outcomes of the present study can be summarized as follows:

1. The effect of nanofluid parameters, i.e. Nb , Nt , Le , Nv and Nc , on the non-dimensional velocity and temperature profiles is comparatively negligible. However, the variation of Nb , Nt and Le would significantly affect the concentration profiles. Therefore, in the case of variable thermal conductivity and variable viscosity, i.e. $Nv=0.1$ and $Nc=0.1$, the

variation of volume fraction of nanoparticles strongly affects the surface heat transfer through the variation of thermo-physical properties.

2. An increase of the thermophoresis parameter (Nt) or decrease of Brownian motion parameter (Nb) would decrease the volume fraction of nanoparticles at the surface. The high values of thermophoresis parameter would lead to zero volume fraction of nanoparticles at the surface. An augmentation of Lewis number would raise the volume fraction of nanoparticles at the surface (would decrease the concentration difference between the free stream and the surface).
3. The enhancement ratio between the nanofluid and base fluid ($h_{drift-flux}/h_{bf}$) shows that using nanofluids may not always enhance the heat transfer. In some cases, the heat transfer from the plate may be reduced about -7% by using nanofluids. However, in some cases, the heat transfer may be increased about 22% by using nanofluids. Therefore, adjusting the non-dimensional parameters of nanofluids (by adjusting the size and type of nanoparticles or other available design parameters) to increase the convective heat transfer of nanofluids is crucial.
4. The enhancement ratio, $h_{drift-flux}/h_{hom}$, between the non-homogenous model of nanofluids (drift-flux model) and the homogenous model, reveals that the enhancement of nanofluids using homogenous models may be underestimated about 14%. However, in some cases, the homogenous model may overestimate the heat transfer enhancement about 5%.

6. NOMENCLATURE

(x, y)	Cartesian coordinates
C	Specific heat (J/ kg. K)
D_B	Brownian diffusion coefficient (m^2/s)
D_T	Thermophoretic diffusion coefficient (m^2/s)
F	Rescaled nanoparticles volume fraction, nanoparticles concentration
H	Convective heat transfer coefficient (J/m^2)
J	Drift flux
K	Thermal conductivity (W/ m K)
Le	Lewis number
Nb	Brownian motion parameter
Nc	Variable thermal conductivity parameter
Nr	Buoyancy ratio
Nt	Thermophoresis parameter
Nv	Variable viscosity parameter
P	Pressure (Pa)
Pr	Prandtl number
Re_x	Local Reynolds number
S	Dimensionless stream function
T	Temperature (K)
u, v	x and y velocity components (m/s)
V	Velocity

Greek Symbols

(ρc)	Heat capacity ($J/m^3 K$)
μ	Viscosity (Pa s)
A	Thermal diffusivity (m^2/s)
H	Dimensionless distance
Θ	Dimensionless temperature
N	Cinematic viscosity
P	Density (kg/m^3)
ϕ	Nanoparticles volume fraction
ψ	Stream function

Subscripts

∞	Free stream
Bf	The base fluid
<i>drift-flux</i>	The drift flux model
<i>Hom</i>	The homogenous model
<i>Nf</i>	Nanofluid
<i>P</i>	Nanoparticles
<i>W</i>	Plate, wall, surface

7. ACKNOWLEDGEMENT

The first and second authors acknowledge the financial support of Dezful Branch, Islamic Azad University, Dezful, Iran and Iran Nanotechnology Initiative Council (INIC) for the support of the present study.

8. REFERENCE

- [1] S. Kakaç, A. Pramuanjaroenkij, Review of convective heat transfer enhancement with nanofluids, *International Journal of Heat and Mass Transfer*, 52 (2009) 3187-3196.
- [2] K. Khanafer, K. Vafai, A critical synthesis of thermophysical characteristics of nanofluids, *International Journal of Heat and Mass Transfer*, 54 (2011) 4410-4428.
- [3] S.K. Das, S. Choi, W. Yu, T. Pradeep, *Nanofluids: science and technology*, Wiley Interscience, New Jersey, 2007.
- [4] R. Saidur, K.Y. Leong, H.A. Mohammad, A review on applications and challenges of nanofluids, *Renewable and Sustainable Energy Reviews*, 15 (2011) 1646-1668.
- [5] N. Bachok, A. Ishak, I. Pop, Boundary-layer flow of nanofluids over a moving surface in a flowing fluid, *International Journal of Thermal Sciences*, 49 (2010) 1663-1668.
- [6] J. Buongiorno, Convective Transport in Nanofluids, *Journal of Heat Transfer*, 128 (2006) 240-245.
- [7] A. Noghrehabadi, R. Pourrajab, M. Ghalambaz, Effect of partial slip boundary condition on the flow and heat transfer of nanofluids past stretching sheet prescribed constant wall temperature, *International Journal of Thermal Sciences*, 54 (2012) 253-261.
- [8] N.A. Yacob, A. Ishak, R. Nazar, I. Pop, Falkner–Skan problem for a static and moving wedge with prescribed surface heat flux in a nanofluid, *International Communications in Heat and Mass Transfer*, 38 (2011) 149-153.
- [9] N. Bachok, A. Ishak, I. Pop, Flow and heat transfer characteristics on a moving plate in a nanofluid, *International Journal of Heat and Mass Transfer*, 55 (2012) 642-648.
- [10] A. Noghrehabad, M. Ghalambaz, M. Ghalambaz, A. Ghanbarzadeh, Comparison between thermal enhancement of ag-water and sio2-water nanofluids over an isothermal stretching sheet with suction or injection, *Journal of Computational and Applied Research in Mechanical Engineering*, 2 (2012) 35-47.
- [11] A.J. Chamkha, A.M. Aly, MHD Free Convection Flow of a Nanofluid past a Vertical Plate in the Presence of Heat Generation or Absorption Effects.” *Chemical Engineering Communications*, 198 (2011) 425-441.
- [12] G.K. Ramesh, A. J. Chamkha, and B.J. Gireesha, Magnetohydrodynamic Flow of a Non-Newtonian Nanofluid Over an Impermeable Surface with Heat Generation/Absorption, *Journal of Nanofluids*, 3 (2014) 78-84.
- [13] A. J. Chamkha and S.M.M. El-Kabeir, Unsteady Heat and Mass Transfer By MHD Mixed Convection Flow Over an Impulsively Stretched Vertical Surface with Chemical Reaction and Soret and Dufour Effects, *Chemical Engineering Communications*, 200 (2013) 1220-1236, 2013.
- [14] A. J. Chamkha and A. M. Rashad, MHD Forced Convection Flow of a Nanofluid Adjacent to a Non-Isothermal Wedge, *Computational Thermal Sciences*, 6 (2014) 27-39, 2014.
- [15] P.V. Murthy, C. RamReddy, A.J. Chamkha and A.M. Rashad, Significance of Viscous Dissipation and Chemical Reaction on Convective Transport in a Boundary Layer Stagnation Point Flow Past a Stretching/Shrinking Sheet in a Nanofluid, *Journal of Nanofluids*, 4 (2014) 214-222.

- [16] N.G. Rudraswamy, B.J. Gireesha and A.J. Chamkha, Effects of Magnetic Field and Chemical Reaction on Stagnation-Point Flow and Heat Transfer of a Nanofluid over an Inclined Stretching Sheet, *Journal of Nanofluids*, 4 (2015) 239-246, 2015.
- [17] A. Noghrehabadi, R. Pourrajab, M. Ghalambaz, Flow and heat transfer of nanofluids over stretching sheet taking into account partial slip and thermal convective boundary conditions, *Heat and Mass Transfer*, (2013) 1-10.
- [18] A. Noghrehabadi, M. Ghalambaz, A. Ghanbarzadeh, Heat Transfer of Magnetohydrodynamic Viscous Nanofluids over an Isothermal Stretching Sheet, *Journal of thermophysics and heat transfer*, 26 (2012) 686-689.
- [19] J.C. Maxwell, *A Treatise on Electricity and Magnetism*, Clarendon Press, Oxford, UK, second edition, (1881).
- [20] H.C. Brinkman, 571 (1952). The Viscosity of Concentrated Suspensions and Solutions, *Journal of Chemical Physics*, 20 (1952) 571.
- [21] S. Kakac, A. Pramaumjaroenkij, Review of convective heat transfer enhancement with nanofluids, *Int. J. Heat Mass Transfer*, 52 (2009) 3187–3196.
- [22] J. Buongiorno, D.C. Venerus, N. Prabhat, T. McKrell, J. Townsend, R. Christianson, et al., A Benchmark Study on the Thermal Conductivity of Nanofluids, *J Appl Phys*, 106 (2009) 094312.
- [23] D.C. Venerus, J. Buongiorno, R. Christianson, J. Townsend, I.C. Bang, G. Chen, et al., Viscosity Measurements on Colloidal Dispersions (Nanofluids) for Heat Transfer Applications, *Applied Rheology*, 20(2010) 44582.
- [24] L.F. Shampine, J. Kierzenka, M.W. Reichelt, Solving boundary value problems for ordinary differential equations in MATLAB with bvp4c, Tutorial notes, (2000).
- [25] J.R. Lloyd, E.M. Sparrow, Combined forced and free convection flow on vertical surfaces, *International journal of heat and mass transfer*, 13 (1970) 434-438.
- [26] G. Wilks, Heat-transfer coefficients for combined forced and free convection flow about a semi-infinite, isothermal plate, *International Journal of Heat and Mass Transfer*, 19 (1976) 951-953.
- [27] A. Ishak, R. Nazar, I. Pop, Flow and heat transfer characteristics on a moving flat plate in a parallel stream with constant surface heat flux, *Heat Mass Transfer*, 45 (2009) 563-567.
- [28] H. Curtis, *bital mechanics for engineering students*, 2 ed., Butterworth-Heinemann, United States of America, 2009.

Appendix A

Using the boundary layer approximations, the momentum equations, Eq. (2), is written as:

$$\rho_{nf} \left(u \frac{\partial u}{\partial x} + v \frac{\partial u}{\partial y} \right) = \frac{\partial \left(\mu_{nf}(\phi) \frac{\partial u}{\partial y} \right)}{\partial y} \quad (A1)$$

which can be rewritten as:

$$\rho_{nf} \left(u \frac{\partial u}{\partial x} + v \frac{\partial u}{\partial y} \right) = \frac{\partial \mu_{nf}(\phi)}{\partial y} \frac{\partial u}{\partial y} + \frac{\mu_{nf}(\phi)}{\mu_{nf,\infty}} \frac{\partial^2 \left(\frac{\partial u}{\partial y} \right)}{\partial y^2} \quad (A2)$$

where using similarity variables:

$$\frac{\partial \eta}{\partial y} = \frac{\text{Re}_x^{\frac{1}{2}}}{x}, \quad \text{and} \quad \frac{\partial \eta}{\partial x} = -\frac{1}{2} \frac{\eta}{x}, \quad (A3)$$

$$v = v_{nf} \frac{1}{2} \frac{\text{Re}_x^{\frac{1}{2}}}{x} (\eta S' - S) \quad (\text{A4})$$

$$u = U_\infty S' \quad (\text{A5})$$

The other terms of Eq. (A2) have been obtained as:

$$\frac{\partial u}{\partial x} = \frac{\partial u}{\partial S'} \frac{\partial S'}{\partial \eta} \frac{\partial \eta}{\partial x} = -\frac{1}{2} \frac{\eta}{x} U_\infty S'' \quad (\text{A6})$$

$$\frac{\partial u}{\partial y} = \frac{\partial u}{\partial S'} \frac{\partial S'}{\partial \eta} \frac{\partial \eta}{\partial y} = \frac{\text{Re}_x^{\frac{1}{2}}}{x} U_\infty S'', \quad \frac{\partial^2 u}{\partial y^2} = \frac{\partial u}{\partial S''} \frac{\partial S''}{\partial \eta} \frac{\partial \eta}{\partial y} = U_\infty \frac{\text{Re}_x}{x^2} S''' \quad (\text{A7})$$

$$\frac{\partial \frac{\mu_{nf}(\phi)}{\mu_{nf,\infty}}}{\partial y} = \frac{\partial \eta}{\partial y} \frac{\partial \left(\frac{\mu_{nf}(\phi_\infty f + \phi_\infty)}{\mu_{nf,\infty}} \right)}{\partial \eta} \quad (\text{A8})$$

Substituting Eqs. (A4-A8) in Eq. (A2) yields

$$\begin{aligned} \rho_{nf} \left(-\frac{1}{2} \frac{\eta}{x} U_\infty S'' U_\infty S' + v_{nf} \frac{1}{2} \frac{\text{Re}_x^{\frac{1}{2}}}{x} (\eta S' - S) \frac{\text{Re}_x^{\frac{1}{2}}}{x} U_\infty S'' \right) \\ = \frac{\text{Re}_x^{\frac{1}{2}}}{x} \frac{\partial \mu_{nf}(\phi_\infty f + \phi_\infty)}{\partial y} \frac{\text{Re}_x^{\frac{1}{2}}}{x} U_\infty S'' + \mu_{nf}(\phi_\infty f + \phi_\infty) U_\infty \frac{\text{Re}_x}{x^2} S''' \end{aligned} \quad (\text{A9})$$

Simplifying Eq. (A9) leads to Eq. (10).

Using typical boundary layer assumptions, Eq. (3), in the Cartesian system, is written as

$$(\rho c)_{nf} \left(u \frac{\partial T}{\partial x} + v \frac{\partial T}{\partial y} \right) = k_{nf,\infty} \frac{\partial \left(\frac{k_{nf}(\phi)}{k_{nf,\infty}} \right)}{\partial y} \frac{\partial T}{\partial y} + k_{nf,\infty} \left(\frac{k_{nf}(\phi)}{k_{nf,\infty}} \right) \frac{\partial^2 T}{\partial y^2} + (\rho c)_p \left[D_B \frac{\partial \phi}{\partial y} \frac{\partial T}{\partial y} + \frac{D_T}{T_\infty} \left(\frac{\partial T}{\partial y} \right)^2 \right] \quad (\text{A10})$$

where:

$$\frac{\partial T}{\partial y} = \frac{\partial T}{\partial \theta} \frac{\partial \theta}{\partial \eta} \frac{\partial \eta}{\partial y} = (T_w - T_\infty) \theta' \frac{\text{Re}_x^{\frac{1}{2}}}{x}, \quad \frac{\partial^2 T}{\partial y^2} = \frac{\partial T}{\partial \theta'} \frac{\partial \theta'}{\partial \eta} \frac{\partial \eta}{\partial y} = (T_w - T_\infty) \frac{\text{Re}_x}{x^2} \theta'' \quad (\text{A11})$$

$$\frac{\partial \phi}{\partial y} = \frac{\partial \phi}{\partial f} \frac{\partial f}{\partial \eta} \frac{\partial \eta}{\partial y} = \phi_\infty f' \frac{\text{Re}_x^{\frac{1}{2}}}{x} \quad (\text{A12})$$

$$\frac{\partial T}{\partial x} = \frac{\partial T}{\partial \theta} \frac{\partial \theta}{\partial \eta} \frac{\partial \eta}{\partial x} = -\frac{1}{2}(T_w - T_\infty) \frac{\eta}{x} \theta' \quad (\text{A13})$$

$$\frac{\partial \frac{k_{nf}(\phi)}{k_{nf,\infty}}}{\partial y} = \frac{\partial \eta}{\partial y} \frac{\partial \left(\frac{k_{nf}(\phi_\infty f + \phi_\infty)}{k_{nf,\infty}} \right)}{\partial \eta} \quad (\text{A14})$$

Substituting Eqs. (A4-A7) and Eqs. (A11-A14) into Eq. (A9) yields:

$$\begin{aligned} (\rho c)_{nf} \left(-\frac{1}{2} \frac{\eta}{x} (T_w - T_\infty) \theta' U_\infty S' + \frac{1}{2} v_{nf} \frac{\text{Re}_x^{\frac{1}{2}}}{x} (\eta S' - S) (T_w - T_\infty) \theta' \frac{\text{Re}_x^{\frac{1}{2}}}{x} \right) \\ = \frac{\partial \eta}{\partial y} \frac{\partial k_{nf}(f)}{\partial \eta} \frac{\partial T}{\partial y} + k_{nf}(f) \frac{\partial^2 T}{\partial y^2} + (\rho c)_p \left[D_B \phi_\infty f' \frac{U_\infty}{v_\infty} \frac{1}{x} (T_w - T_\infty) \theta' + \frac{D_T}{T_\infty} \frac{U_\infty}{v_\infty} \frac{1}{x} (T_w - T_\infty)^2 \theta'^2 \right] \end{aligned} \quad (\text{A15})$$

Simplifying Eq. (A15) leads to Eq. (11).

The conservation of nanoparticles, Eq. (4), is written as:

$$\left[u \frac{\partial \phi}{\partial x} + v \frac{\partial \phi}{\partial y} \right] = D_B \frac{\partial^2 \phi}{\partial y^2} + \left(\frac{D_T}{T_\infty} \right) \frac{\partial^2 T}{\partial y^2}, \quad (\text{A16})$$

where

$$\frac{\partial \phi}{\partial x} = \frac{\partial \phi}{\partial f} \frac{\partial f}{\partial \eta} \frac{\partial \eta}{\partial x} = -\frac{1}{2} \frac{\eta}{x} \phi_\infty f', \quad \frac{\partial^2 \phi}{\partial y^2} = \frac{\partial \phi}{\partial f'} \frac{\partial f'}{\partial \eta} \frac{\partial \eta}{\partial y} = \phi_\infty f'' \frac{\text{Re}_x}{x^2} \quad (\text{A17})$$

Substituting Eqs. (A4), (A5), (A11), (A12), (A17) into Eq. (A16) yields:

$$\left[-\frac{1}{2} \frac{\eta}{x} \phi_\infty f' U_\infty S' + v_{nf} \frac{\text{Re}_x^{\frac{1}{2}}}{x} (\eta S' - S) \phi_\infty f' \frac{\text{Re}_x^{\frac{1}{2}}}{x} \right] = D_B \phi_\infty f'' \frac{\text{Re}_x}{x^2} + \left(\frac{D_T}{T_\infty} \right) (T_w - T_\infty) \frac{\text{Re}_x}{x^2} \theta', \quad (\text{A18})$$

Simplifying Eq. (A18) leads to Eq. (12). Using Eqs. (17-a) and (17-b), the terms $\frac{\mu_{nf}(f)}{\mu_\infty}$,

$$\left(\frac{\mu_{nf}(f)}{\mu_\infty} \right)', \frac{k_{nf}(f)}{k_\infty} \text{ and } \left(\frac{k_{nf}(f)}{k_\infty} \right)' \text{ are obtained as } \frac{k_{nf}}{k_{nf,\infty}} = 1 + Nc f, \left(\frac{k_{nf}}{k_{nf,\infty}} \right)' = Nc f',$$

$$\frac{\mu_{nf}}{\mu_{nf,\infty}} = 1 + Nv f \text{ and } \left(\frac{\mu_{nf}}{\mu_{nf,\infty}} \right)' = Nv f'.$$